ELSEVIER

Journal of Alloys and Compounds 275–277 (1998) 450–454

Journal of ALLOYS AND COMPOUNDS

Theoretical study on complex f–f transition simulation of luminescence spectra of nanocrystalline X_1–Y_2SiO_5:Eu^{3+} [1]

C. Duan[a,b,*], S. Xia[a,b,c], W. Zhang[b], M. Yin[b], J.-C. Krupa[d]

[a] *Structure Research Lab, University of Science and Technology of China, Academia Sinica, Hefei, 230026, P.R. China*
[b] *Department of Physics, University of Science and Technology of China, Hefei, 230026, P.R. China*
[c] *State Key Lab of Rare Earth Materials Chemistry and Applications, Beijing, 100871, P.R. China*
[d] *Radiochimie, Institute de Physique Nucleaire, B.P. No. 1, 91406, Orsay, France*

Abstract

Based on the electrostatic crystal-field model of M. Faucher, in which the induced electric dipoles of ligands are obtained from a set of self-consistent combined equations and the contributions from far ligands are considered, the crystal-field energy parameters of nanocrystalline X_1–Y_2SiO_5:Eu^{3+} at two sites both with C_1 symmetry are calculated by using related data of its crystal structure and physical properties. Moreover, we successfully extend the above model to calculate the transition intensities, therefore giving a computed simulation of luminescence spectroscopy consistent with the experimental one which we measured before, supporting the model and the data we adopted here. © 1998 Published by Elsevier Science S.A.

Keywords: Luminescence; f–f transition; Crystal-field parameters

1. Introduction

Y_2SiO_5:Eu^{3+} was found to be a promising candidate for coherent time-domain optical memory applications [1]. We have studied experimentally the photoluminescence properties of nanocrystalline X_1–Y_2SiO_5:Eu^{3+} [2]. We present here an analysis of the experimental results.

Y_2SiO_5 is polymorphous and the X_1 and X_2 types crystallize in monoclinic space groups $P2_1/c$ and $B2/b$, respectively, depending on the synthesis temperature [3,4]. In either of these two crystals, Eu^{3+} may occupy two different crystallographic sites. All four sites have the same C_1 site symmetry but the coordination numbers of the two sites of X_1 type are 7 and 9, while they are 6 and 7 for X_2 type. In X_1–Y_2SiO_5:Eu^{3+}, the luminescent center Eu^{3+} substitutes for Y^{3+} resulting in two kinds of different luminescent centers Eu(1) and Eu(2). The low C_1 site symmetry makes it impossible to apply a parameter fitting because there are too many parameters. Therefore, we adopted a model calculation based on the self-consistent electrostatic scheme developed by Faucher [5,6]. In addition, to decrease the unreasonable values of intensity parameters A^2_{1p} ($p=1,0,-1$), we introduced decaying–shielding factors in our calculation.

As the results of the calculation, we got the crystal field and intensity parameters, the theoretically simulated spectra and wavefunctions which could be used for the calculation of other physical properties. Moreover, the values of model parameters we adopted are physically meaningful.

2. Model theory

In Refs. [5,6] the consistent electrostatic model (hereafter referred to as CEM) was utilized to calculate the crystal-field energy parameters of a rare-earth (RE) ion embedded in a crystal lattice. In this scheme, the crystal-field parameters can be written as:

$$A_{kq} = A_{kq}(\mathrm{P}) + A_{kq}(\mathrm{D}), \tag{1}$$

where $A_{kq}(\mathrm{P})$ and $A_{kq}(\mathrm{D})$ are contributions from point charge $C_j e$ and from induced dipoles $\vec{M}_j$ of surrounding ions, respectively:

*Corresponding author.

[1] Supported by National Science Foundation of China and by special foundation for doctorial program of National Education Committee of China.

0925-8388/98/$19.00
PII: S0925-8388(98)00366-1

$$A_{kq}(\mathrm{P}) = -\sqrt{\frac{4\pi}{2k+1}}\, e^2 \sum_j \frac{C_j}{R_j^{k+1}}\, Y_q^{k*}(\alpha_j,\beta_j), \tag{2}$$

$$A_{kq}(D) = -\sqrt{\frac{4\pi}{2k+1}}\, e \sum_j \vec{M}_j \cdot \vec{\nabla}\left(\frac{Y_q^{k*}(\alpha_j,\beta_j)}{R_j^{k+1}}\right), \tag{3}$$

where $(R_j,\ \alpha_j,\ \beta_j)$ are the spherical coordinates of the jth ligand and the summations in Eqs. (2) and (3) are performed over all the ions surrounding the RE ion.

Moreover, under a simplified hypothesis of isotropic polarizability $\bar{\alpha}$, the induced dipole $\vec{M}_j$ of the jth surrounding ion is calculated self-consistently and can be written as:

$$\vec{M}_j = \bar{\alpha}_j \vec{E}_j, \tag{4}$$

while the electric field $\vec{E}_j$ on ion j is produced by both the point charges and the point dipoles of other ions:

$$\vec{E}_j = \sum{}' \vec{\nabla}_{j'}\left(\frac{C_j' e}{R_{jj'}}\right) + \sum{}' \vec{\nabla}_{j'}\left[\vec{M}_{j'} \cdot \vec{\nabla}_{j'}\left(\frac{1}{R_{jj'}}\right)\right]. \tag{5}$$

From Eqs. (4) and (5), we can get a linear self-consistent system with $M_{j\nu}$ ($\nu=1,2,3$) as the variables. In a crystal (as in our case), the ions occupying ''equivalent'' crystallographic sites have the same dipoles due to translational invariance. Thus $j=1,2,\ldots,n$, where n is the number of ions in a primitive cell. When we calculated the summations $\Sigma'\vec{\nabla}_{j'}(C_{j'}/R_{jj'})$ and $\Sigma'\vec{\nabla}_{j'}\vec{\nabla}_{j'}(C_{j'}/R_{jj'})$, we utilized the Ewald method [5–10] by which the summations converge fast and accurate results are easier to obtain.

The usual effective crystal-field parameters B_k^q are:

$$B_k^q = A_{kq}\langle r^k\rangle = B_k^q(\mathrm{P}) + B_k^q(\mathrm{D}), \tag{6}$$

where $\langle r^k\rangle$ are the expectation values of r^k in one-electron radial wavefunctions and have been given in [11]. B_k^q were corrected by multiplying by two factors: $\gamma(k)$ [5,6] and $[1-\sigma(k)]$ [12], where $\gamma(k)$ is the correction factor for $\langle r^k\rangle$ and $\sigma(k)$ is the shielding factor (Table 1).

The intensity parameter A_{tp}^{λ} is made up of two parts [7–9]:

$$A_{tp}^{\lambda} = A_{tp}^{\lambda}[\mathrm{SC}] + A_{tp}^{\lambda}[\mathrm{DC}]. \tag{7}$$

(1) $A_{tp}^{\lambda}[\mathrm{SC}]$ is the contribution of the static coupling between the central ion and ligands:

$$A_{tp}^{\lambda}[\mathrm{SC}] = A_{tp}\Xi(t,\lambda)\frac{2\lambda+1}{\sqrt{2t+1}}\ \ (\lambda = 2,4,6\ \text{ and }\ t = \lambda\pm 1), \tag{8}$$

Table 1
Correction coefficients of $\langle r^k\rangle$ and shielding parameters

k	2	4	6
$\sigma(k)$	0.6865	0.1390	0.109
$\gamma(k)$	1.40	2.0	2.6

where the values of $\Xi(t,\lambda)$ for Eu^{3+} used in our calculation were taken from Ref. [13]. (2) $A_{tp}^{\lambda}[\mathrm{DC}]$ is the contribution of the dynamic coupling between the central ion and ligands, where $\lambda=2,4,6$ and $t=\lambda+1$ (in Judd–Ofelt fitting theory, this mechanism is included automatically). Assuming that the ligands have an isotropic polarizability, we have [7–9,14]:

$$A_{tp}^{\lambda}[\mathrm{DC}] = 7\begin{pmatrix} 3 & \lambda & 3 \\ 0 & 0 & 0 \end{pmatrix}\sqrt{(\lambda+1)(2\lambda+1)}\langle r^{\lambda}\rangle \times(-1)^p\gamma(\lambda)(1-\sigma(\lambda))\ \delta_{t,\lambda+1}\sum_j C_{-p}^{(\lambda+1)}(\vec{r}_j)R_j^{-(\lambda+2)}\bar{\alpha}_j. \tag{9}$$

We recognized that a correction should be made for A_{tp}^{λ} in the above calculation, especially for the contribution to A_{1p}^2 of those ligands who are 1 nm or farther from Eu^{3+}. By this crude analysis we multiplied the jth term by a factor $\exp((r_{\min}-R_j)/r_0)$, and took $r_0=1$ nm and $r_{\min}$ as the average bond length of Eu–O. By this we mainly decreased the effect of distant ligands, which only corrects A_{1p}^2 significantly and makes it converge quickly. It is reasonable to smooth out the distant interactions since in fact there are thermal vibrations and defects which have not been considered. Besides, all the ligands contribute an electric field $E_p(0)=A_{1p}/e$ (where $p=1,0,-1$ are the index of a vector in spherical base coordination) on the central ion. To keep the electric field on the center ion zero, the electrons of it are polarized, generating a shielding electric field $E_p'(0)=-A_{1p}/e$, which will affect the f-electrons at inner orbits so that the A_{1p} in Eq. (8) that the f-electrons ''felt'' decrease greatly. By a crude fit to the relative intensity of spectra, we introduced a multiplier $[1-\sigma(1)]$ to A_{1p} and chose the shielding factor $\sigma(1)=0.8$, which describes a stronger shielding effect for $t=1$ than for $t=2$ since $\sigma(2)=0.69$.

As a comparison, we give the scheme proposed by M.F. Reid [7–9] (hereafter referred as STM), in which only the nearest neighbors of the central ion are taken into account in Eq. (2) for $A_{kq}(\mathrm{P})$, and the induced dipoles at ligands are considered to be affected only by the central ion:

$$A_{kq}[\mathrm{D}] = 2(-1)^q e^2 C(k+1)\sum_i \bar{\alpha}_i C_{-q}^{(k)}(\theta_i,\phi_i)R_i^{-(k+4)},$$

where C is the charge of the RE ion and i is the index of ligand.

We made a program to calculate the parameters and then applied M.F. Reid's program to calculate the energy level and intensity, in which the magnetic dipole contribution is considered in the usual way.

3. Application to X_1–Y_2SiO_5:Eu^{3+}

Table 2 gives the structural parameters of X_1–Y_2SiO_5 (space group $P2_1/c$). Each primitive cell of this crystal has 32 atoms, whose coordinates can be derived by $\pm(x,\ y,\ z;$

Table 2
Atom position parameter, charge and polarizability of each atom of X_1–Y_2SiO_5:Eu^{3+}

	$a=6.790$	$b=9.142$	$c=7.054$	$\beta=107.52$	
	x	y	z	C	α
Si	0.2020	0.5876	0.4598	+3	0.2
Y(1)	0.52458	0.62451	0.23428	+3	0.2
Y(2)	0.11453	0.1460	0.41628	+3	0.2
O(1)	0.2032	0.4302	0.6453	−1.8	2.0
O(2)	0.1317	0.4587	0.2520	−1.8	2.0
O(3)	0.3839	0.6361	0.5059	−1.8	2.0
O(4)	0.0941	0.7681	0.4507	−1.8	2.0
O(5)	0.3837	0.3782	0.0487	−1.8	2.0

Note that the ionic properties of different rare earth elements are almost the same. Here we take the atom position parameters of X_1–Gd_2SiO_5 instead in the absence of that of X_1–Y_2SiO_5. Unit: *a*,*b*,*c*: 0.1 nm, β: angle degree.

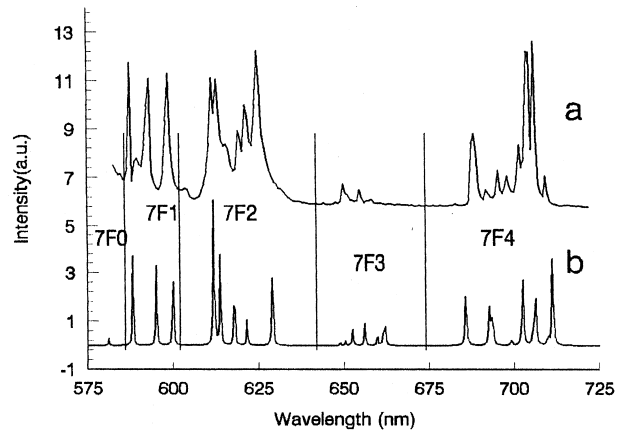

Fig. 2. (a) Experimental emission spectrum and (b) theoretical spectrum of site 1.

x, $1/2-y$, $z+1/2$). The physical parameters of each ion were ascribed the following values: crystal Y_2SiO_5 is a strongly ionized isolator and so as to keep the primitive cell neutral we set $C_{Si}=3.0$, $C_Y=3.0$, and $C_O=-1.8$, which is comparable with Refs. [7–9,15] where set $C_O=-2.0$ and $C_O=-1.55$, respectively. The polarizability of a cation is usually smaller than that of an anion by one or two order(s) of magnitude so it is reasonable to set $\alpha_Y=\alpha_{Si}=0.2\times(0.1\text{ nm})^3$ (or zero, which has no obvious effect on the results), and $\alpha_O=2\times(0.1\text{ nm})^3$ [5,6].

The observed emission spectra of nanocrystalline X_1–Y_2SiO_5:Eu^{3+} at 300 K excited by a 254 nm Hg lamp are composed of five groups of lines (Fig. 1), corresponding to transitions from $^5D_0$ to ^7F_j ($j=0,\ldots,4$) multiplets of two different sites. The evidence of Eu^{3+} occupying two sites in Y_2SiO_5:Eu^{3+} is that the two luminescence spectra (Fig. 2(a) and Fig. 3(a)) are selectively excited by different lights (579.7 and 577.7 nm) corresponding to the transitions $^7F_0\rightarrow{}^5D_0$ for the two sites, respectively. And the lifetime of the $^5D_0$ states of site 1 and site 2 are 2.94 and 1.82 ms, respectively.

Based on the calculated parameters B_k^q and A_{tp}^{λ} (see Table 3, where only the three multiplet–multiplet intensity parameters Ω_λ related to A_{tp}^{λ} are listed), the luminescence spectra of Eu(1) or Eu(2) are calculated as shown in Fig. 2(b) and Fig. 3(b), respectively. In the simulation, some adjustment of some quasifree ion parameters were made to fit the positions of the main peaks of the experimental

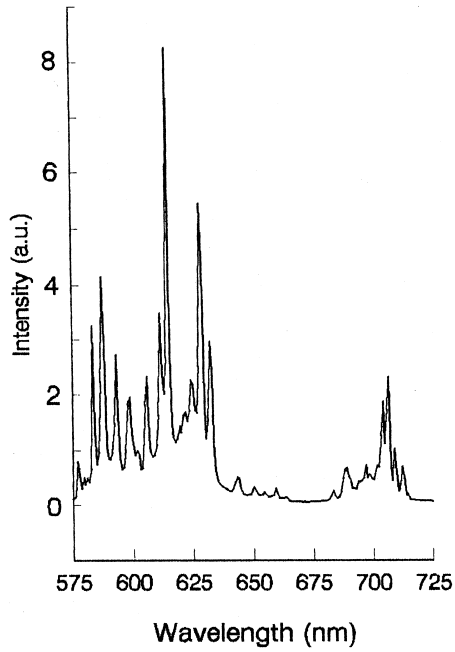

Fig. 1. Luminescence spectra of X_1–Y_2SiO_5:Eu^{3+} under UV excitation at 300 K.

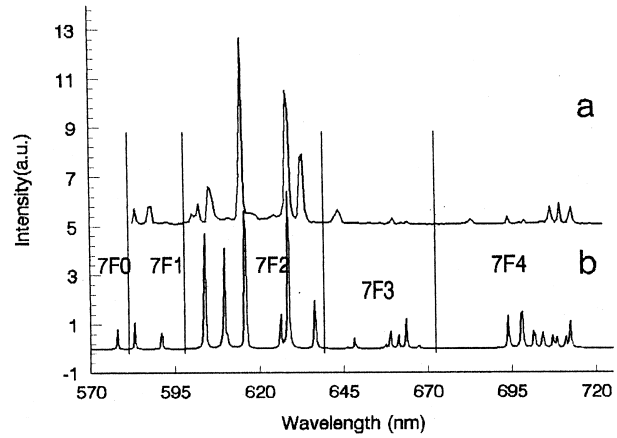

Fig. 3. (a) Experimental emission spectrum and (b) theoretical spectrum of site 2.

Table 3
Calculated crystal field parameter

Parameter	$B(k,q)$ (cm^{-1}), Ω_k (10^{-20} cm^2)	
$B_k^q = B(k,q)$	Site 1	Site 2
$B(2,0)$	−108	1481
$B(2,1)$	−743−i257	446−i14
$B(2,2)$	−65−i744	210+i671
$B(4,0)$	−536	1509
$B(4,1)$	−515+i70	415+i729
$B(4,2)$	−186+i1534	362−i658
$B(4,3)$	134+i141	416−i218
$B(4,4)$	178+i572	248+i118
$B(6,0)$	−455	−39
$B(6,1)$	26−i72.	133−i129
$B(6,2)$	78−i144	86+i108
$B(6,3)$	22+i100	15+i159
$B(6,4)$	−377−i135	9+i35
$B(6,5)$	39−i108	85
$B(6,6)$	−174+i117	−16−i70
Ω_2	0.5	2.3
Ω_4	1.2	2.0
Ω_6	3.4	6.1

spectra, as shown in Table 4. It was decided that sites Eu(1) and Eu(2) were related to spectra 1 and 2, respectively, and therefore the coordination numbers of the Eu ions of spectra 1 and spectra 2 were equal to 7 and 9, respectively. This assigment is supported by the following discussion.

Our theoretical results of the Eu(1) site agree quite well with the experimental results: (1) the calculated relative intensity and energy position of each peak belonging to $^5D_0 \rightarrow {}^7F_{1,2}$ transition agrees quite well with experiment, as seen in Fig. 2(a,b), (2) the theoretical intensities of the $^5D_0 \rightarrow {}^7F_3$ transitions agree with the experimental result qualitatively in that both of them are very weak. Although the calculated intensity distribution of the $^5D_0 \rightarrow {}^7F_4$ transition is slightly different from the observation, the calculated total intensity of the $^5D_0 \rightarrow {}^7F_4$ transition almost equals that of the $^5D_0 \rightarrow {}^7F_2$ transition, which is consistent with the experimental result.

As for the Eu(2) site, we also got reasonable results: the intensity ratio of the $^5D_0 \rightarrow {}^7F_0$ transition to the shortest-wavelength transition of $^5D_0 \rightarrow {}^7F_1$ is 2/3 while the experimental result is 1/2; the calculated strong peaks of the $^5D_0 \rightarrow {}^7F_2$ transition are consistent with the experimental ones. So are the intensities of $^5D_0 \rightarrow {}^7F_{3,4}$. In addition, the theoretical calculation shows that the intensity of the $^5D_0 \rightarrow {}^7F_4$ transition is much smaller than that of $^5D_0 \rightarrow {}^7F_2$ for Eu(2), which is opposite to Eu(1). It is just the same in the experimental spectrum. Besides, we know the transition probability of the main peak of $^5D_0 \rightarrow {}^7F_2$ is determined by Ω_2. The calculated Ω_2 of Eu(2) is bigger than that of Eu(1). This is compatible with the fact that the decay time of Eu(2) (1.82 ms) is shorter than that of Eu(1) (2.84 ms).

Table 4
Values of quasifree ion energy parameters used in this calculation (unit: cm^{-1})

Site	F^2	F^4	F^6	ξ_{nl}
1	83 582	59 586	41 241	1318
2	83 682	59 686	41 341	1351

We also did the same simulation by the STM but failed to give reasonable results (especially, the parameters B_2^q and A_{1p}^2 even have different signs compared to the ones obtained in CEM) even though we made adjustments on effective charges and polarizabilities.

In conclusion, we carried out a computational simulation on the peak position and intensity of the luminescence spectra of nanocrystalline $X_1-Y_2SiO_5:Eu^{3+}$, utilizing the CEM and the STM, respectively. We got the following main results: (1) two sites observed from experiment, site 1 and site 2, correspond to Eu in Y(1) (7 coordinations) and Y(2) (9 coordinations), respectively. (2) We got reasonable energy parameters and spectral peak positions by the CEM. The STM, not including the self-consistent calculation of the important induced dipole and the contribution from the distant interaction, failed to give a reasonable result. (3) We used CEM to calculate A_{tp} in the transition intensity parameters A_{tp}^{λ}(SC) and got an intensity distribution well consistent with observation when the decaying–shielding factors were introduced. The STM scheme also failed here for the same reason as stated above. (4) The calculated transition probability of site 2 is much greater than that of site 1, which is consistent with experimental results. (5) Although there is covalency in nanocrystalline X_1–$Y_2SiO_5:Eu^{3+}$, the electrostatic model is effective when the above covalency correction is adopted. (6) In our case of nanocrystalline $X_1-Y_2SiO_5:Eu^{3+}$, nanometric effects affect only energy transfer and concentration quenching (see our paper, Refs. [2,16]), while energy levels and transition probabilities do not seem to be much concerned with nanometric effects.

References

[1] M. Mitsunaga, R. Yano, N. Uesugi, Opt. Lett. 16 (1991) 1890.
[2] M. Yin, W. Zhang, S. Xia, J.-C. Krupa, J. Lumin. 68 (1996) 335.
[3] Joint Committee on Powder Diffraction Standard (JCPDS) (ASTM), File No. 41-4.
[4] Joint Committee on Powder Diffraction Standard (JCPDS) (ASTM), File No. 21-1456.
[5] M. Faucher, J. Dexpert-Ghys, P. Caro, Phys. Rev. B 21 (1980) 3689.
[6] M. Faucher, J. Dexpert-Ghys, P. Caro, Phys. Rev. B 27 (1983) 7386.
[7] M.F. Reid, F.S. Richardson, J. Chem. Phys. 79 (1983) 5735.
[8] M.F. Reid, J. Dallara, F.S. Richardson, J. Chem. Phys. 79 (1983) 5743.
[9] M.F. Reid, F.S. Richardson, J. Phys. Chem. 88 (1984) 3579.
[10] Charles Kittel, Introduction to Solid State Physics, 6th ed., Wiley, 1986.

[11] A.J. Freeman, R.E. Watson, Phys. Rev. 127 (1962) 2058.
[12] J. Dexpert-Ghys, M. Faucher, P. Caro, Phys. Rev. B 23 (1981) 607.
[13] W.F. Krupke, Phys. Rev. 145 (1966) 325.
[14] B.R. Judd, J. Chem. Phys. 70 (1979) 4830.
[15] C.A. Morrison, D.E. Wortman, N. Karayianis, J. Phys. C 9 (1976) L191; N. Karayianis and C.A. Morrison, U.S. National Technical Report Information Service, Springfield Va., Report No. A011252.
[16] W. Zhang, P. Xie, C. Duan, et al., Preparation and Size Effect on Concentration Quenching of Nanocrystalline Y_2SiO_5:Eu, submitted to Chemical Physics letters.